Pulse-Response Study for the Humidity Effect on Sorption of Ethyl Bromide on Clays

Nail Yaşyerli and Gülşen Doğu
Dept. of Chemical Engineering, Gazi University, Ankara, Turkey

Timur Doğu
Dept. of Chemical Engineering, Middle East Technical University, Ankara, Turkey

B. J. McCoy
Dept. of Chemical Engineering, University of California, Davis, CA 95616

The effects of relative humidity on sorption and the diffusion of ethyl bromide in kaolinite and montmorillonite pellets were investigated by the one-sided single-pellet moment technique. Montmorillonite demonstrated a higher water affinity than kaolinite, causing a sharper decrease of the ethyl bromide adsorption equilibrium constant with an increase of relative humidity. For montmorillonite, most of the active sites are covered by water even at relative humidities of 8%, and adsorption of ethyl bromide on the gas–water interface controls the sorption process. For kaolinite, however, adsorption on gas-to-mineral, gas-to-water, and water-to-mineral surfaces contributes to the sorption process. Effective macropore diffusivity of ethyl bromide in montmorillonite showed a decreasing trend with increase in relative humidity. This is due to high water uptake of montmorillonite and the corresponding change in pore structure. No such change was observed for kaolinite.

Introduction

Contamination of soil subsurface and groundwater by volatile organic compounds (VOCs) is a major environmental problem. Adsorption of chlorinated and brominated volatile hydrocarbons in soil has attracted significant attention in the literature (Chiou and Shoup, 1985; Thibaud et al., 1992; Cabbar et al., 1994).

Adsorption on the mineral surface and partitioning into the soil organic matter significantly retard the migration of volatile organic pollutants in soil. The type of clay, moisture, and organic content of the soil determines the sorption capacity and also the migration rate (Unger et al., 1996; Batterman et al., 1995; Chiou et al., 1988; Valsaraj and Thibodeaux, 1988). In the presence of moisture, water is expected to compete with VOC for sorption on the mineral surface, and consequently to reduce the sorption of gaseous organic species (Smith et al., 1990; Rao et al., 1989).

Depending upon the moisture content and the composition of the soil, water may exist as films covering pore surfaces, it may fill the micropores of the clay minerals and even macropores of the soil aggregates, and it may be adsorbed or condensed, blocking the pore mouths. In the work of McCoy and Rolston (1992) four different mathematical models were presented for partially saturated soil aggregates based on capillary tubes, porous and nonporous particles, and porous particles with water-filled pores.

In the analysis of sorption of organic gases onto a partially saturated soil, adsorption onto dry mineral surfaces, dissolution into adsorbed water films, and adsorption on the gas–water and water–solid interfaces should be considered. In the recent work of Unger et al. (1996) different possible mechanisms of sorption onto a moist soil were discussed. In many cases, linear equilibrium relations were assumed for VOC adsorption on the gas–mineral surfaces, and Henry's law was used for dissolution into the liquid film.

Condensation of organic vapors in the micropores and partitioning into soil organic matter should also be considered in the modeling of the sorption process (Pennell et al., 1992; Chiou and Shoup, 1985). In the recent paper of Pignatello and Xing (1996) rate-limiting factors that determine the sorp-

Correspondence concerning this article should be addressed to T. Doğu.

tion rate of organic chemicals to natural particles were critically reviewed. Diffusion through the natural organic-matter matrix and diffusion through intraparticle micropores of nanometer size contribute to the slow sorption of organic vapors on soil. In the case of thick water films and water-filled micropores, hindered diffusion of organic species may also be a rate-determining step in the adsorption and desorption processes.

Swelling of some clays, such as montmorillonite, is another important factor influencing the transport and sorption of organic vapors in soil (Chen et al., 1987). Pore structure of montmorillonite was shown to change considerably with an increase of total surface area in the presence of water due to swelling (Altın, 1997).

Gas chromatography techniques are frequently used for the investigation of adsorption parameters. One of the earliest articles on packed-bed chromatography for the investigation of adsorption equilibrium and rate parameters was by Schneider and Smith (1968). Thibaud et al. (1992) developed a frontal analysis chromatography technique to investigate the adsorption equilibria of volatile organics on soil. They determined adsorption isotherms of several organic contaminants with this procedure. More recently, the single-pellet moment technique, originally developed for the investigation of diffusion and adsorption in catalyst pellets (Doğu and Smith, 1975, 1976) was modified and applied to investigate adsorption and diffusion of volatile organic contaminants in soil (Cabbar et al., 1994, 1996; Doğu et al., 1993). In these studies reversible and irreversible adsorption of benzene and some chlorinated volatile hydrocarbons on dry clay and clay–humic acid complexes was investigated.

The new one-sided single-pellet moment technique proposed by Doğu et al. (1996) was shown to be an effective method for the investigation of adsorption in soil pellets. In the present study, this one-sided single-pellet dynamic procedure was modified to investigate adsorption and pore diffusion of ethyl bromide in different clays (kaolinite and montmorillonite) at different relative humidities.

One-Sided Single-Pellet Moment Method

In this technique, a porous adsorbent (soil) pellet is placed into the one-sided single-pellet adsorption cell (Figure 1). The upper-end face of the pellet is exposed to a flow of an inert gas (helium). The cell is designed so that the chamber above the pellet is perfectly mixed and the film mass-transfer resistance between the gas and the upper face of the pellet is negligible. Details of the method and the single-pellet cell are published elsewhere (Doğu et al., 1996). For the evaluation of adsorption parameters, pulses of an adsorbing tracer (ethyl bromide in the present work) were injected into the carrier gas flowing through the upper chamber and the response peaks were detected in the exit stream. Then the moments of the response peaks were used for the evaluation of adsorption equilibrium and rate parameters on the porous sorbent.

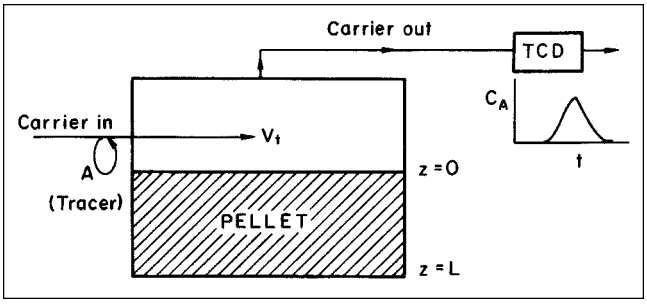

Figure 1. The one-sided single-pellet adsorption cell.

Experimental values of the moments were determined by the numerical integration of Eq. 1,

$$m_n = \int_0^\infty t^n C_A \, dt. \tag{1}$$

First and second moment values also include contributions due to dead volumes in the injection and detection lines. To correct for these contributions pulse-response experiments were repeated with an impermeable Teflon plate placed over the pellet, and the moments corresponding to the top chamber were also determined (Doğu et al., 1996).

Moment expressions derived for inert, reversibly, and irreversibly adsorbed tracers were reported before (Doğu et al., 1996). In several adsorption studies with soils, a local adsorption equilibrium assumption was made for the fluid and adsorbed phase concentrations. Some of the adsorption–desorption processes are rather slow and some irreversible adsorption is also possible (Doğu et al., 1993). Within the time scale of a pulse-response experiment, reversible and irreversible adsorption processes may simultaneously take place at different sites in the soil matrix. For such a case, the species conservation equation within the porous soil pellet can be expressed as

$$(\epsilon_p + \rho_p K_i)\frac{\partial C_i}{\partial t} = D_e \frac{\partial^2 C_i}{\partial z^2} - \rho_p k_a C_i. \tag{2}$$

Here, the linear adsorption equilibrium and linear irreversible adsorption rate (second term on the righthand side) relations are assumed. At low concentrations of tracers such linear adsorption relations are usually justified. The boundary conditions and species conservation equation in the upper chamber are the same as reported by Doğu et al. (1996).

For an adsorbing tracer (simultaneous reversible and irreversible adsorption) the zeroth moment expression (m_0), which corresponds to the area under the response curve, is

$$\frac{m_{0t}}{m_0} = 1 + \left(\frac{1}{F}\right)\left(\frac{D_e A}{L}\right)(\zeta L)\tanh(\zeta L), \tag{3}$$

where

$$(\zeta L) = L\left(\frac{\rho_p k_a}{D_e}\right)^{1/2} \quad \text{(adsorption Thiele modulus)} \tag{4}$$

and

$$m_{0t} = C_0 \tau = C_0 \frac{V_t}{F} \quad \text{(zeroth moment for the upper chamber)}. \tag{5}$$

The values of m_{0t} may either be found from pulse-response experiments conducted with a Teflon plate covering the upper face of the pellet or may be calculated using C_0V_t determined from the slope of $1/m_0$ vs. F. In the absence of irreversible adsorption, the second term on the righthand side of Eq. 3 becomes zero and (m_{0t}/m_0) approaches unity. For negligible values of the irreversible adsorption rate constant, the deviation of m_{0t}/m_0 from unity is within the experimental error limits. For negligible irreversible adsorption, the corrected first absolute moment (time delay of the response curve) and second central moment expressions are (Doğu et al., 1996),

$$\mu_{1c} = \mu_1 - \mu_{1t} = \frac{AL}{F}(\epsilon_p + \rho_p K_i) \tag{6}$$

$$\mu_{2c} = \mu_2 - \mu_{2t} = \left(\frac{m_2}{m_0} - \left(\frac{m_1}{m_0}\right)^2\right) - \tau^2$$

$$= \left(\frac{AL}{F}\right)(\epsilon_p + \rho_p K_i)\left[2\tau + \left(\frac{AL}{F}\right)(\epsilon_p + \rho_p K_i)\right] + \frac{2}{3}\left(\frac{AL^3}{FD_e}\right)(\epsilon_p + \rho_p K_i)^2 \tag{7}$$

Here,

$$\mu_{1t} = \frac{m_{1t}}{m_{0t}} = \tau \tag{8}$$

is the first absolute moment corresponding to the top chamber (upper surface of the pellet being covered with a Teflon plate). The relation between corrected first absolute moment (μ_{1c}) and $1/F$ is linear, and the slope of this relation may be used for the evaluation of the adsorption equilibrium constant. In the absence of irreversible adsorption, the effective diffusivity may then be evaluated from the second moment data using Eq. 7.

Experimental Work

Dynamic sorption studies were carried out with ethyl bromide tracer and two different clays. The first type of natural clay was montmorillonite, whose chemical composition and some other properties are reported in a previous publication (Doğu et al., 1996). The second type of clay was kaolinite. The crystal structure of the clay was characterized by X-ray diffraction (XRD) analysis of air-dried and ethylene-glycolated samples.

Cylindrical pellets 3 cm in diameter and 0.41 cm in length were prepared from oven-dried clay by pressing into a ring-shaped stainless-steel mold. Pellet surface areas were measured by nitrogen adsorption in a Quantachrome Monosorb apparatus. Pore-size distributions were determined with a Quantachrome 60 mercury intrusion porosimeter. The physical properties of the pellets are summarized in Table 1. The cumulative pore-area distributions of montmorillonite and kaolinite pellets are given in Figure 2. These surface-area distributions were obtained by the mercury intrusion technique and correspond to pores larger than 1.75 nm (macropores). For clays (especially for montmorillonite), bimodal pore-size distributions and some micropores smaller than 1.75 nm are expected. Surface-area values of oven-dried samples obtained by the nitrogen adsorption technique are also given in Table 1. These values correspond to pores of radii smaller than 0.85 nm. Comparison of these values with the surface-area values obtained from the mercury intrusion porosimeter showed larger surface-area values from nitrogen adsorption. This also indicates the presence of pores with radii smaller than 1.75 nm.

Table 1. Physical Properties of the Pellets

	Montmorillonite	Kaolinite
Surface area (m^2/g) (nitrogen adsorption)	58.7	21.7
Apparent density (g/cm^3)	1.25	1.40
Total porosity	0.55	0.49
Surface area (m^2/g) (mercury porosimeter, pores having radii greater than 1.75 nm)	48.0	16.2

In the pulse-response experiments with the one-sided single-pellet sorption cell, the flow rate of the helium carrier gas was in the range 1.85–5.5 cm^3/s. The volume of the upper cell chamber is 7.43 cm^3. Pulse-response experiments were carried out at 30°C by injecting 1.0 μL ethyl bromide tracer into the upper chamber. For experiments at different relative humidities, the humidity of the carrier gas was adjusted by splitting the stream into desired proportions and passing one stream through a water saturator. Saturated and dry streams were then mixed. All the lines between the saturator and the adsorption cell were heated to 30°C to eliminate condensation. A three-way valve was used to introduce this gas into the adsorption cell or to a trap containing magnesium perchlorate. The change of weight of the magnesium perchlorate

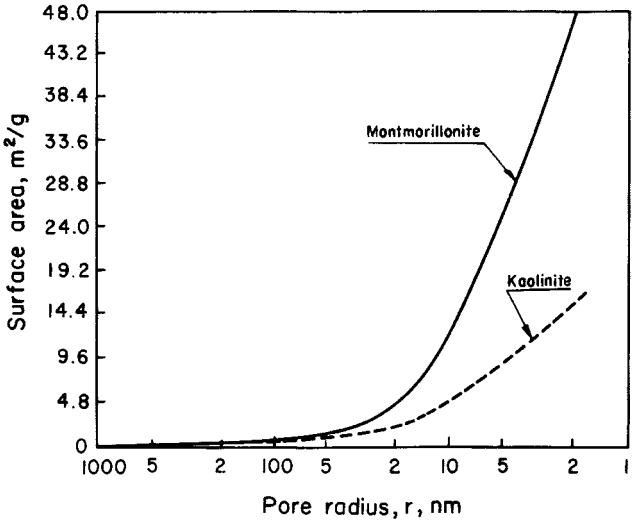

Figure 2. Surface-area distributions of the pellets (mercury-intrusion porosimeter data).

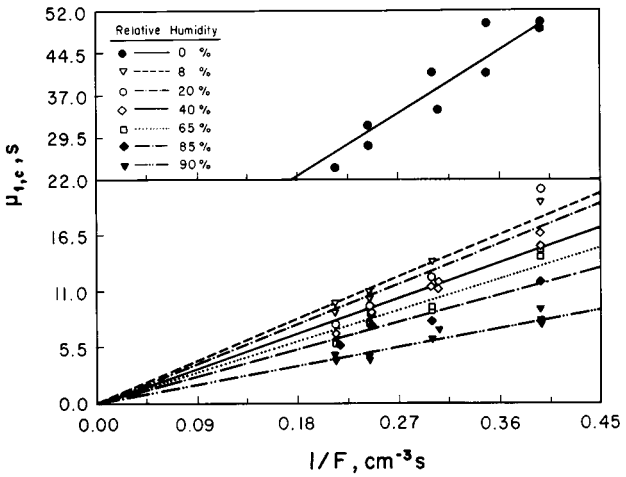

Figure 3. First absolute moment data for ethyl bromide in the montmorillonite pellet ($T = 30$°C).

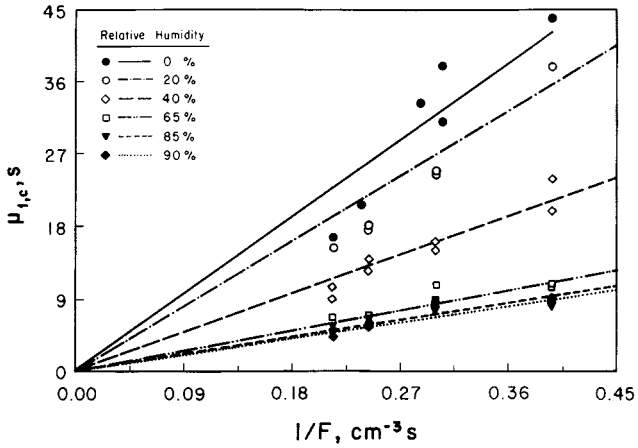

Figure 4. First absolute moment data for ethyl bromide in the kaolinite pellet ($T = 30$°C).

during a certain time period was used to measure the relative humidity of the stream. Pulse-response experiments were then carried out at 0, 8, 20, 40, 65, 85 and 90% relative humidities. The pellet was dried at 105°C in flowing helium after each set of experiments. At each relative humidity about 3 h were allowed prior to pulse-response experiments to ensure that equilibration was reached between the pellet and the humid carrier gas. This equilibration was experimentally checked by the humidity analysis of feed and effluent streams.

Sorption of Ethyl Bromide on Montmorillonite and Kaolinite at Different Relative Humidities

Results of pulse-response experiments conducted at 30°C with ethyl bromide tracer showed that for both montmorillonite and kaolinite, the m_0/m_{0t} values were very close to unity at all relative humidities. Since the deviation of m_0/m_{0t} values from unity was within experimental error limits, sorption was thus reversible within the time scale of the pulse-response experiments.

The corrected first absolute moment data obtained with montmorillonite and kaolinite pellets at different relative humidities are given in Figure 3 and 4, respectively. A major difference was observed for the relative-humidity dependence of the first absolute moments with these two different clay minerals. With kaolinite, a gradual decrease of first absolute moments was observed with an increase in relative humidity. This indicates a gradual decrease of the adsorption equilibrium constant of ethyl bromide with humidity. After a relative humidity of 65%, first absolute moments do not change much. On the other hand, for montmorillonite a very sharp decrease of the first absolute moment values was observed between 0% and 8% relative humidities. After 8% relative humidity, the decrease of first absolute moments with an increase of relative humidity is much less. These results are reflected in the adsorption equilibrium constants. Adsorption equilibrium constants for ethyl bromide on kaolinite and montmorillonite pellets were determined from the slopes of μ_{1c} vs. $1/F$ relations passing through the origin (Eq. 6). The linear dependence of first absolute moments to inverse flow rate is illustrated in Figures 3 and 4. Although there is some scatter, linear trends are experimentally observed. The adsorption equilibrium constants and the R values of linear regression obtained from this analysis are given in Table 2. The adsorption equilibrium constants found here agreed well with the adsorption equilibrium constants reported by Cabbar et al. (1994) for chlorinated hydrocarbons. Cabbar et al. reported the $\rho_p K_i$ value of monochloroethane as 56 on a soil pellet composed of illite- and kaolinite-type clays. The corresponding $\rho_p K_i$ values found in this work are 35.7 and 41.9 for ethyl bromide on kaolinite- and montmorillonite-type clays. Thibaud et al. (1992) reported adsorption data for different volatile organics on soil by a frontal analysis chromatography technique. The uptake data reported for methylene chloride were quite linear and the $\rho_p K_i$ value can be estimated from these data. The estimated value of $\rho_p K_i$ for methylene chloride on a soil sample containing 28.9% clay, 56.4% sand and 14.7% silt is around 5. The order of magni-

Table 2. Comparison of Ethyl Bromide Sorption on Kaolinite and Montmorillonite at Different Relative Humidities ($T = 30$°C)

% Relative Humidity	Kaolinite					Montmorillonite			
	$\rho_p K_i$	R	S^* (m^2/g)	d	f	$\rho_p K_i$	R	S^* (m^2/g)	$\rho_p K_i/S$
0	35.7	0.969	21.7	1	1	41.9	0.980	58.7	0.71
8	—	—	—	—	—	15.2	0.986	46.0	0.33
20	30.1	0.930	17.9	0.98	0.81	14.6	0.961	41.9	0.35
40	17.9	0.979	14.6	0.53	0.36	12.6	0.991	38.8	0.33
65	9.1	0.980	12.6	0.03	0.02	10.9	0.972	34.2	0.32
85	7.6	0.976	9.9	—	—	9.8	0.993	25.0	0.39
90	7.5	0.975	8.3	—	—	6.3	0.974	20.2	0.31

* Determined from nitrogen adsorption sorptometer.

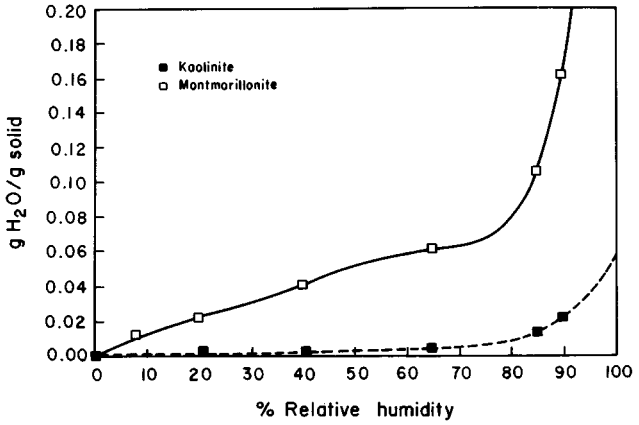

Figure 5. Water uptake of the two clays at different relative humidities.

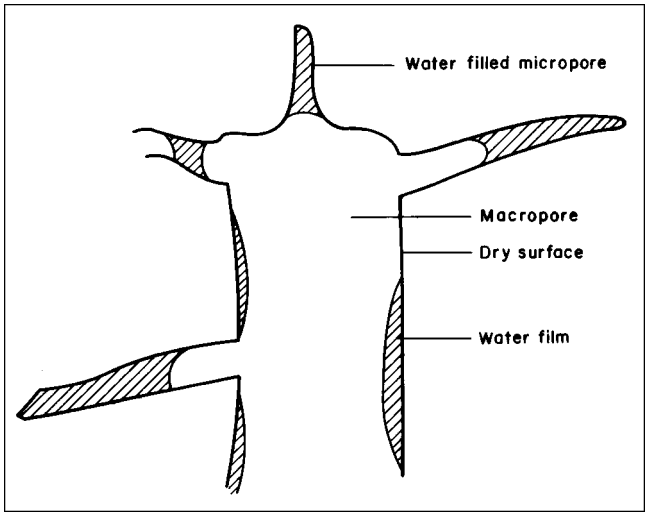

Figure 6. Partially saturated pore structure.

tude agreement for $\rho_p K_i$ values for pure clay and for soil is deemed satisfactory.

As shown in Table 2, $\rho_p K_i$ for montmorillonite at 8% relative humidity is about three times smaller than the corresponding value at 0% relative humidity. The decrease of $\rho_p K_i$ is much less for kaolinite. Water molecules cover a fraction of the mineral surface, and consequently reduce the gas to the mineral surface area, causing a decrease of adsorption of organic species on the mineral surface. Water affinities of clays are quite different. Montmorillonite is known to have a high affinity for water, which penetrates into the micropores of the montmorillonite crystals and causes swelling. For comparison, the water uptake values of the two clays were determined from the weight change at different relative humidities. Results shown in Figure 5 illustrate that there is a significant difference in the water uptake values. The water uptake values of montmorillonite are about an order of magnitude higher than the corresponding values for kaolinite.

Surface areas of the clay samples exposed to carrier gas at different relative humidities were measured with a flow-through single-point sorptometer (Quantachrome Monosorb). For this purpose crushed clay was placed into the cell of the sorptometer and the moist gas (prepared at the desired relative humidity) flowed over this sample until steady state was reached. Then, by means of a three-way valve this moist gas stream was replaced by a dry stream containing 30% nitrogen in helium, and the sorption experiment was conducted at liquid nitrogen temperature. The surface-area values determined by this procedure are also reported in Table 2. The porous matrix exposed to the carrier gas at a certain relative humidity is illustrated in Figure 6. Depending upon the type of clay and the relative humidity of the gas, a fraction of the pore surfaces is covered by a water layer. In addition, some of the micropores are filled with water. The surface area (S) values measured at different relative humidities correspond to the summation of gas-to-mineral surface area (S_{gm}) and gas-to-liquid (S_{gl}) surface area

$$S = S_{gm} + S_{gl}. \tag{9}$$

This area is not the same as the summation of gas-to-mineral and liquid-to-mineral surface area,

$$S_0 = S_{gm} + S_{lm}. \tag{10}$$

For kaolinite, the value of S_0 is expected to be the same as the surface area of the dry clay. For montmorillonite, however, the value of S_0 may increase with relative humidity due to swelling. The decrease of the surface area (S) values reported in Table 2 with an increase in relative humidity is due to the decrease or pore radii with the formation of water film on the pore surfaces and also due to the filling of the micropores.

The monolayer water adsorption capacities of kaolinite and montmorillonite were estimated by fitting the data reported in Figure 5 to the BET equation. For kaolinite, a monolayer coverage of the surface by water molecules corresponds to a water uptake value of about 2×10^{-3} g water/g clay. Such a water uptake value corresponds to a relative humidity of about 39%. This result shows that below 39% relative humidity kaolinite has both dry and wet areas on its surface. At higher relative humidity most of the surface is covered by water molecules and some of the micropores are filled by water. Of course, if the surface coverage with water is not uniform, then some dry surface is possible, even at high relative humidities.

The behavior observed with montmorillonite is quite different. Even at very low relative humidities water uptake is higher than a monolayer adsorption capacity. From the BET equation, the relative humidity corresponding to the monolayer adsorption capacity was estimated to be about 10%. Consequently, for montmorillonite most of the pore surfaces can be assumed to be covered by water even at the lowest values of relative humidity. This is the major reason for the sharp decrease of the ethyl bromide adsorption equilibrium constant on montmorillonite even at very low relative humidities. Different behavior of adsorption equilibrium constants determined at different relative humidities for the two types of clay minerals is due to the differences in water affinity of kaolinite and montmorillonite.

For a model involving adsorption on the dry gas–mineral surface, gas–water surface, dissolution and diffusion in the water layer covering the pore surfaces, and adsorption on the liquid–mineral surface, the adsorption equilibrium constant ($\rho_p K_i$) which appears in the first moment expression becomes

$$\rho_p K_i = \rho_p \left[K_{gm} S d + K_{gl} S (1-d) + \frac{V_l}{K_H} + \frac{K_{lm}}{K_H} (S_0 - S d) \right]. \quad (11)$$

Here, d and V_l correspond to the dry fraction of the measured surface area S (m^2/g) and water uptake (m^3 H_2O/g clay), respectively. The value of dimensionless Henry constant K_H was 8.2 for ethyl bromide (Jury et al., 1990). The values of $[(V_l \rho_p)/K_H]$ calculated using the water uptake data given in Figure 5 showed that this term is at least two orders of magnitude smaller than the corresponding value of $\rho_p K_i$ for both types of clay. This result indicated that the effect of tracer dissolution in the water layer is negligible for ethyl bromide in the first moment analysis. For 0% relative humidity ($d = 1$) the adsorption equilibrium constant at the gas–mineral surface $\rho_p K_{gm}$ is determined as 1.65 $g \cdot m^{-2}$ and 0.71 $g \cdot m^{-2}$ for kaolinite and montmorillonite, respectively. For montmorillonite the $\rho_p K_i/S$ values (Table 2) are nearly uniform at all relative humidities except for 0% relative humidity. As discussed earlier, most of the sorption sites may be covered by water molecules, even at a 8% relative humidity for montmorillonite. For this case, Eq. 11 reduces to

$$\frac{\rho_p K_i}{S} = \rho_p K_{gl} + \frac{\rho_p K_{lm}}{K_H} \frac{S_0}{S} \quad (\text{montmorillonite RH} \geq 8\%). \quad (12)$$

The observation that $\rho_p K_i/S$ is constant (independent of S) at all relative humidities shows the significance of the gas–liquid (K_{gl}) adsorption equilibrium constant as compared to the liquid–mineral (K_{lm}/K_H) adsorption. These results indicate that, for montmorillonite, adsorption at the liquid-to-mineral surface may be neglected. As discussed earlier, a rather thick layer of water covers the pore surfaces for montmorillonite and also the K_H value is quite high for ethyl bromide. The thick layer of water causes a significant resistance for diffusion, and the tracer cannot reach the liquid–mineral surface within the time scale of a pulse-response experiment. The average value of the adsorption equilibrium constant at the gas–water interface is then evaluated as $\rho_p K_{gl} = 0.34$ $g \cdot m^{-2}$.

The adsorption equilibrium constant for ethyl bromide on kaolinite was almost constant for relative-humidity values greater than 85% (Table 2 and Figure 7). Assuming $d = 0$ at relative humidities of 90% and 85%, and using the same gas–water adsorption equilibrium constant as for montmorillonite, the adsorption equilibrium constant at the water–mineral surface was determined from Eq. 12. In the case of kaolinite the water layer is thin and some penetration of ethyl bromide through this layer and adsorption on the water–mineral surface is possible. The average value of the adsorption equilibrium constant at the water–mineral surface was thus estimated as $\rho_p K_{lm} = 1.68$ $g \cdot m^{-2}$. The dry fraction of the measured surface area (d) for kaolinite was calculated from Eq. 11 with the adsorption-equilibrium and surface-area values reported in Table 2. (Results are also given in Table 2.) The experimental and calculated values of $\rho_p K_i$ (using Eq. 11 with the sorption parameters given in Table 2 at different relative humidities) are shown in Figure 7. The dry fraction of the surface area of the original clay S_0 may be calculated from $f = d(S/S_0)$. Values of f calculated from this relation are smaller than d (Table 2), especially at lower relative humidities. This also indicates filling of micropores by water even at low relative humidities.

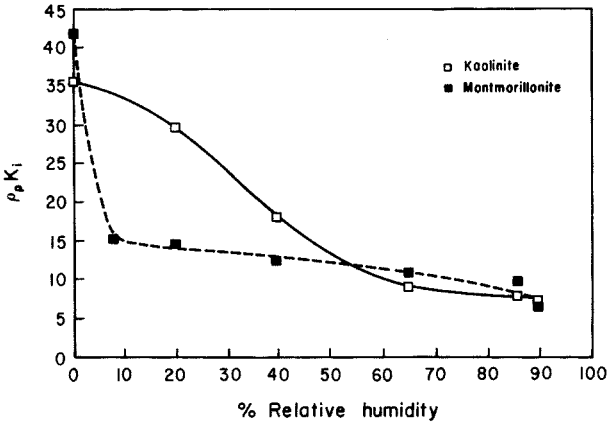

Figure 7. Variation of adsorption equilibrium constant of ethyl bromide with respect to relative humidity.

Effective Diffusivity of Ethyl Bromide in Kaolinite and Montmorillonite

The second moment data obtained for ethyl bromide with montmorillonite and kaolinite pellets are given in Figures 8

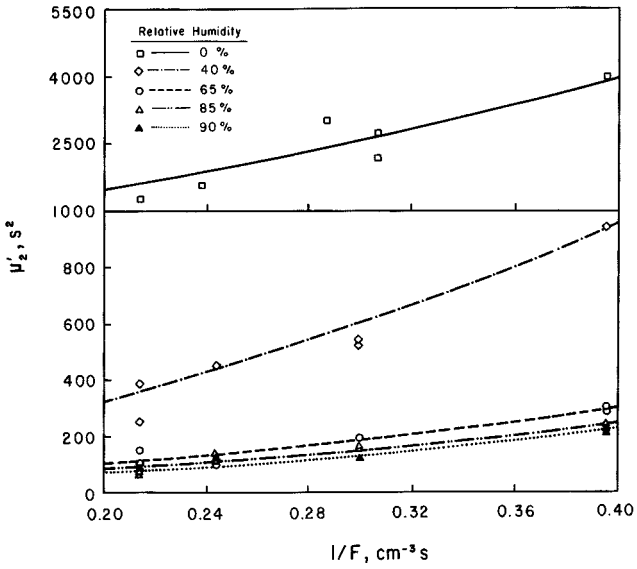

Figure 8. Second central moment data for ethyl bromide in kaolinite.

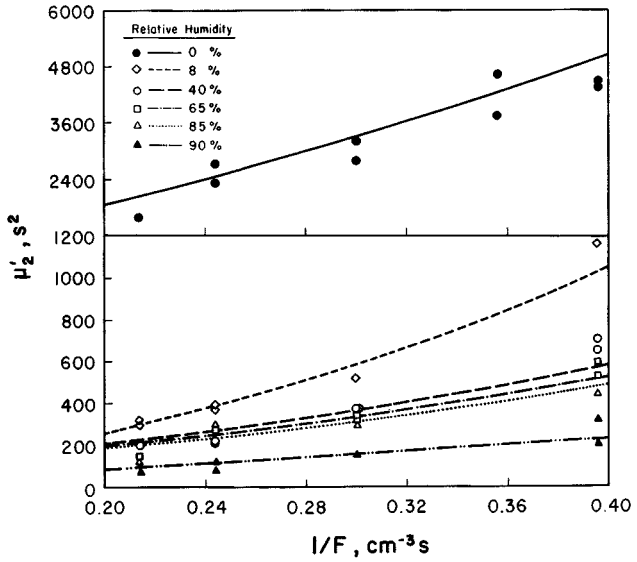

Figure 9. Second central moment data for ethyl bromide in montmorillonite.

and 9, respectively. Knowing the adsorption equilibrium constants from the first moment analysis (Table 2), effective macropore diffusion coefficients were evaluated from the second moment data obtained at different relative humidities. In this analysis Eq. 7 was used and results are given in Table 3. Second moment data are generally more scattered than the first moment data, and this affects the accuracy of effective diffusivity. The R values of regression in second moment data analysis ranged between 0.825 and 0.938. The value of effective macropore diffusivities reported here agree well with the diffusivity values obtained by different techniques (Cabbar et al., 1994; Doğu, 1998).

The effective macropore diffusivity values measured in kaolinite at different relative humidities are almost constant at around 0.11 cm^2/s. This result indicates that there is practically no significant change in the macropore structure of kaolinite at different relative humidities. On the other hand, effective diffusivity values show a decreasing trend with relative humidity for montmorillonite. As was discussed in the previous sections, water uptake of montmorillonite was high. With an increase of relative humidity, a significant increase of water uptake was observed. Due to capillary condensation of water, the particle porosity decreases and the tortuosity increases. Also, some swelling of microporous montmorillonite particles was expected in the presence of water (Chen et al., 1987; Altın, 1997; Altın et al., 1998).

Table 3. Effective Diffusivity of Ethyl Bromide in Kaolinite and Montmorillonite Pellets (D_e, cm^2/s)

% Relative Humidity	Kaolinite	Montmorillonite
0	0.09	0.099
8	—	0.072
40	0.12	0.092
65	0.12	0.066
85	0.10	0.054
90	0.12	0.053

Concluding Remarks

Results of this study showed that detailed information could be obtained about the sorption mechanism of volatile organic contaminants in partially saturated soil using the one-sided single-pellet moment technique. It was found that for montmorillonite and kaolinite pellets, irreversible adsorption of ethyl bromide was negligible within the time scale of pulse-response experiments.

When a clay pellet is exposed to a carrier gas containing some water vapor, a fraction of the pore surface is covered and some of the micropores are filled by water. This caused a significant reduction in the adsorption equilibrium constant of volatile organic tracer. Water affinity on montmorillonite is much higher than kaolinite. At a relative humidity of about 10%, water uptake of montmorillonite corresponds to a monolayer coverage of pores with water. This high water affinity causes a very sharp decrease of the adsorption equilibrium constant of ethyl bromide in montmorillonite. For kaolinite a fraction of the surface is dry unless the relative humidity is very high. Analysis of sorption data for montmorillonite showed that dissolution of ethyl bromide in the water layer and adsorption on the liquid–mineral surface are negligible as compared to adsorption on the gas–water and gas–mineral surfaces. This is mainly due to the large water layer thickness in montmorillonite and also due to the high value of Henry's constant for ethyl bromide. However, for kaolinite the water uptake values are small and the thickness of the water layer is also expected to be small. In this case some contribution of adsorption at the water–mineral surface is also detected.

Acknowledgment

Research Grant NATO CRG 951073 made the collaboration between the parties at Gazi University, METU, and the University of California, Davis, possible and is gratefully acknowledged.

Notation

A = area of the pellet
C_A = concentration of the tracer in the upper chamber
C_i = concentration of the tracer in the pores of the pellet
C_0 = initial concentration of the tracer in the upper chamber
D_e = effective diffusivity in the pores
F = flow rate of carrier gas
$(k_a \rho_p)$ = irreversible adsorption rate constant
$(K_i \rho_p)$ = overall adsorption equilibrium constant
L = pellet length
t = time
V_t = volume of top chamber

Greek letters

ρ_p = pellet density
τ = defined by Eq. 5, $(\tau = V_t/F)$
$\zeta = (\rho_p k_a/D_e)^{1/2}$

Literature Cited

Altın, O., "Removal of Heavy Metals in Wet Soil Matrix," PhD Thesis, Middle East Technical Univ., Ankara, Turkey (1997).
Altın, O., H. O. Özbelge, and T. Doğu, "Use of General Purpose Adsorption Isotherms for Heavy Metal-Clay Mineral Interactions," *J. Colloid Interface Sci.*, **198**, 130 (1998).
Batterman, S., A. Kulshrestha, and H. Cheng, "Hydrocarbon Vapor Transport in Moist Soil," *Environ. Sci. Technol.*, **29**, 171 (1995).
Cabbar, C., G. Doğu, T. Doğu, and B. J. McCoy, "Single Pellet Dy-

namics for the Soil Organic Matter Effect on Dichloroethane Sorption,'' *AIChE J*., **42**, 2090 (1996).
Cabbar, C., G. Doğu, T. Doğu, B. J. McCoy, and J. M. Smith, ''Analysis of Diffusion and Sorption of Chlorinated Hydrocarbons in Soil by Single Pellet Moment Technique,'' *Environ. Sci. Technol*., **28**, 1312 (1994).
Chen, S., P. F. Low, J. H. Cushman, and C. B. Roth, ''Organic Compound Effects on Swelling and Flocculation of Upton Montmorillonite,'' *Soil Sci. Soc. Amer. J*., **51**, 1444 (1987).
Chiou, C. T., D. E. Kile, and R. L. Malcolm, ''Sorption of Vapors of Some Organic Liquids on Soil Humic Acid and Its Relation to Partitioning of Liquid Compounds in Soil Organic Matter,'' *Environ. Sci. Technol*., **22**, 298 (1988).
Chiou, C. T., and T. D. Shoup, ''Soil Sorption of Organic Vapors and Effects of Humidity on Sorptive Mechanism and Capacity,'' *Environ. Sci. Technol*., **19**, 1196 (1985).
Doğu, T., ''Diffusion and Reaction in Catalyst Pellets with Bidisperse Pore Size Distributions,'' *Ind. Eng. Chem. Res*., **37**, 2158 (1998).
Doğu, G., and J. M. Smith, ''A Dynamic Method for Catalyst Diffusivities,'' *AIChE J*., **21**, 58 (1975).
Doğu, G., and J. M. Smith, ''Rate Parameters from Dynamic Experiments with Single Catalyst Pellets,'' *Chem. Eng. Sci*., **31**, 123 (1976).
Doğu, T., C. Cabbar, and G. Doğu, ''Single Pellet Technique for Irreversible and Reversible Adsorption in Soil,'' *AIChE J*., **39**, 1895 (1993).
Doğu, T., N. Yaşyerli, G. Doğu, B. J. McCoy, and J. M. Smith, ''One-Sided Single-Pellet Technique for Adsorption and Intraparticle Diffusion,'' *AIChE J*., **42**, 516 (1996).
Jury, W. A., D. Russu, G. Streile, and H. E. Abd, ''Evaluation of Volatilization by Organic Chemicals Residing Below the Soil Surface,'' *Water Resour. Res*., **26**, 13 (1990).
McCoy, B. J., and D. E. Rolston, ''Convective Transport of Gases in Moist Porous Media: Effect of Absorption, Adsorption and Diffusion in Soil Aggregates,'' *Environ. Sci. Technol*., **26**, 2468 (1992).
Pennell, K. D., R. D. Rhue, P. Suresh, C. Rao, and C. T. Johnston, ''Vapor-Phase Sorption of *p*-Xylene and Water on Soils and Clay Minerals,'' *Environ. Sci. Technol*., **26**, 756 (1992).
Pignatello, J. J., and B. Xing, ''Mechanism of Slow Sorption of Organic Chemicals to Natural Particles,'' *Environ. Sci. Technol*., **30**, 1 (1996).
Rao, P. S. C., R. A. Ogwada, and R. D. Rhue, ''Adsorption of Volatile Organic Compounds on Anhydrous and Hydrated Sorbents: Equilibrium Adsorption and Energetics,'' *Chemosphere*, **18**, 2177 (1989).
Schneider, P., and J. M. Smith, ''Adsorption Rate Constants from Chromatography,'' *AIChE J*., **14**, 767 (1968).
Smith, J. A., C. T. Chiou, J. A. Kammer, and D. E. Kile, ''Effect of Soil Moisture on the Sorption of Trichloroethene Vapor to Vadose-Zone Soil at Picatinny Arsenal, New Jersey,'' *Environ. Sci. Technol*., **24**, 676 (1990).
Thibaud, C., C. Erkey, and A. Akgerman, ''Investigation of Adsorption Equilibria of Volatile Organics on Soil by Frontal Analysis Chromatography,'' *Environ. Sci. Technol*., **26**, 1159 (1992).
Unger, D. R., T. L. Thientu, C. E. Schaefer, and D. S. Kosson, ''Predicting the Effect of Moisture on Vapor-Phase Sorption of Volatile Organic Compounds to Soils,'' *Environ. Sci. Technol*., **30**, 1081 (1996).
Valsaraj, K. T., and L. J. Thibodeaux, ''Equilibrium Adsorption of Chemical Vapors on Surface Soils Landfills and Landfarms—A Review,'' *J. Hazard. Mater*., **19**, 79 (1988).

Manuscript received Mar. 27, 1998, and revision received Oct. 21, 1998.